

# Physical characterization of ZnO precursors

Author: Xavier de la Cruz Romero.

Advisor: Anna Maria Vilà Arbonès.

Facultat de Física, Universitat de Barcelona, Diagonal 645, 08028 Barcelona, Spain.

**Abstract:** Zinc oxide (ZnO) is an important semiconductor material with multiple applications in piezo-electric transducers, spin functional devices and gas sensors, for instance. In this article, we study optical and structural properties of ZnO thin films obtained from 4 precursors deposited by sol-gel on glass substrates and heated to 4 different temperatures each one. The absorption coefficient and energy band gap were determined from UV-visible absorption spectrum (200 – 1100 nm). The luminescence properties were evaluated from photoluminescence spectrum (350 – 850 nm). The amount of impurities in the final material were obtained from elemental analysis. The energy band gap was found to vary between 3.00 – 3.25 eV, depending on the precursor and the annealing temperature. We discuss and relate the different processes with the impurities and structure of the samples. SEM images of the thin films were added to complete the study.

## I. INTRODUCTION

### A. Sample preparation

Regarding the ink preparation, zinc acetate dihydrate from Panreac, 2-metoxoethanol (ME) of the Aldrich brand and different amino alcohols of Acrös Organics like ethanolamine (EA), (S)-(+)-2-amino-1-propanol (Apr), (S)-(+)-2-amino-3-methyl-1-butanol (AMB) and 2-aminobenzyl alcohol (AB) have been used [1]. The reagents used have the molecular structure shown below.

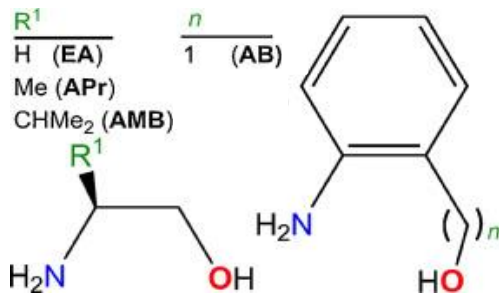


**FIG. 1:** Molecular structure of the aliphatic (left) and aromatic (right) amino alcohols used [1].

The inks were prepared with 0.5 g of ZAD, then treated with an equimolar amount of the corresponding stabilizer (EA, Apr, AMB or AB) and finally 5 ml of solvent (ME) were added. Once the inks were prepared, they were stirred for about 30 minutes and, when ready, they were deposited by sol-gel on the glass substrate and heated to different temperatures: 300 °C, 400 °C, 500 °C and 600 °C [1].

### B. UV-VIS spectroscopy

Ultraviolet-visible (UV-VIS) spectroscopy is one of the most popular analytical techniques because it is very versatile, non-destructive, simple and able to give many optical properties of most materials. With UV-Vis spectroscopy, the UV-VIS light is passed through a sample and the absorbance of light by the sample is measured. A spectrum is obtained that shows the absorbance at different wavelengths, due to the

structure of the molecule [2]. The UV-VIS range used extends from 100 - 1100 nm approximately.

The main mechanism for light absorption in semiconductors is the interband or fundamental absorption, which leads to the generation of electron-hole pairs as a result of optical excitation of electrons from the valence band (VB) to the conduction band (CB). The minimum quantum energy needed to excite electrons from the valence band to the conduction band is equal to the band gap of the semiconductor [3]. This absorption usually occurs in the visible and near ultraviolet spectral range.

The absorption coefficient ( $\alpha$ ) determines how far into a material light of a certain wavelength can penetrate before it is absorbed. Light absorption reduces the transmission of light as it is passed through a sample. Light intensity attenuates exponentially related to the concentration of the sample and light path length travelled. We can obtain that coefficient from absorbance (A) measured and sample thickness (L):

$$T = \frac{I}{I_0} ; A = -\log T = \log\left(\frac{I_0}{I}\right) \quad (1)$$

$$I = I_0 \cdot e^{-\alpha L} \rightarrow \alpha L = \ln\left(\frac{I_0}{I}\right) \quad (2)$$

$$\alpha L = 2,303 \cdot \log\left(\frac{I_0}{I}\right) \rightarrow \alpha = \frac{2,303 \cdot A}{L} \quad (3)$$

Where I is the light intensity, I<sub>0</sub> is the initial light intensity and T is the transmittance.

The band gap energy of the semiconductor can be determined from the spectral dependence of the absorption coefficient for allowed or forbidden transitions [3,4]:

$$\alpha = \frac{\beta(h\nu - E_g)^n}{h\nu} \quad (4)$$

Where  $\beta$  is an absorption constant called band tailing parameter,  $h\nu$  is the photon (light) energy and  $E_g$  is the band gap energy.

The dependence  $n=1/2$  correlates with direct allowed transitions,  $n=3/2$  with direct forbidden transitions,  $n=2$  with indirect allowed transitions and  $n=3$  with indirect forbidden transitions [4].

The Tauc plot shows the quantity  $(\alpha h\nu)^{1/n}$  versus  $h\nu$ . The resulting plot has a distinct linear regime which denotes the

onset of absorption. Thus, extrapolating this linear region to the abscissa yields the energy of the optical band gap of the material.

### C. Elemental analysis

Elemental analysis is a process where a sample of some material is analysed for its elemental and sometimes isotopic composition. This technique can be qualitative if shows what elements are present in the sample or quantitative if determinates how much of each are present. Elemental analysis has different methods. The most common is the CHNX analysis, which is used in this study.

The method is based on the complete and instantaneous oxidation of the sample by flash combustion, which converts all organic and inorganic substances of the sample into combustion products. The resulting combustion gases pass through a furnace with copper to remove the excess of oxygen and to reduce the nitrogen oxides to elemental nitrogen. The resulting mixture is directed by the carrier gas (Helium) to the chromatographic column, where the individual components are separated and eluted as Nitrogen ( $N_2$ ), Carbon dioxide ( $CO_2$ ) and Water ( $H_2O$ ). Then, these gases are detected by a thermal conductivity detector (TCD), which gives an output signal proportional to the concentration of the individual components of the mixture [5].

### D. Photoluminescence

Photoluminescence spectroscopy (PL) is a contactless, non-destructive method of probing the electronic structure of materials. Light is directed onto a sample, where it is absorbed and photo-excitation takes place. This process causes electrons within a material to move into permissible excited states. When these electrons return to their equilibrium states, the excess energy is released and may include the emission of light (a radiative process) or may not (a nonradiative process). The emitted light in this process is photoluminescence and its energy is related to the difference in energy levels between the two electron states involved in the transition: the excited state and the equilibrium state [11]. The intensity of the emitted light is measured by a detector and a spectrum is obtained that shows the material PL at different wavelengths.

UV-vis spectroscopy measures transitions from the ground state to excited state, while photoluminescence deals with transitions from the excited state to the ground state. The greater the absorbance is at a certain wavelength, the more molecules are promoted to the excited state and the more emission will be observed.

Radiative transitions in semiconductors are related to energy band gap and localized defect levels. The photoluminescence energy associated with these levels can be used to identify the band gap of the material as well as specific defects and impurities [12].

### E. Scanning electron microscopy

Scanning electron microscopy (SEM) is a type of electron microscopy that produces images of a sample by scanning the surface with a focused beam of electrons. When the electron beam hits the surface of the sample, it penetrates to a depth of a few microns, depending on the accelerating voltage and the density of the sample. As the electrons interact with atoms in the sample, they produce secondary electrons, backscattered electrons, and characteristic X-rays [16]. These signals are collected by one or more detectors to form images which are then displayed on a screen. SEM images can be used to obtain information about the surface topography, morphology, composition and crystallinity of a material.

## II. RESULTS AND DISCUSSION

Regarding UV-VIS spectroscopy, 3 different absorbance measurements have been used to analyse each sample. This means we have 3 absorbance spectra for every ZnO precursor at each annealing temperature. As explained in the introduction, we have done the appropriate transformation from absorbance data to obtain the absorption coefficient dependence, and then, represent the Tauc plot. Representative figures for absorbance spectrum and Tauc plot are shown below.

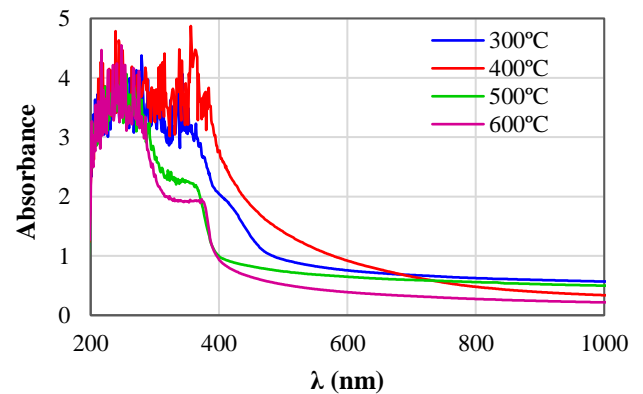


FIG 2. Absorbance spectrum for AB at each annealing temperature.

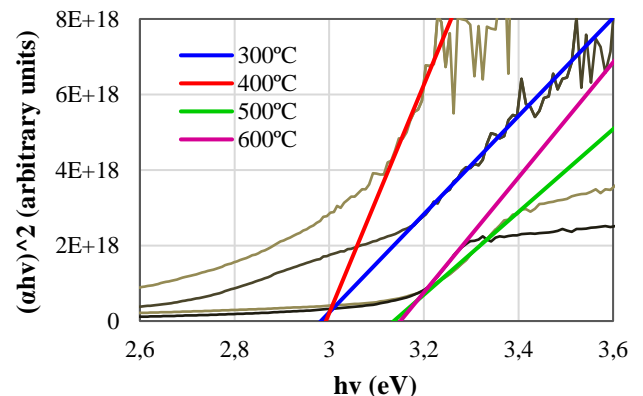


FIG. 3: Tauc plot for AB at each annealing temperature.

From Tauc plot we have determined the corresponding energy band gap. Some uncertainty has been added due to lack of precision in the linear extrapolation and error propagation. We can also assert that all ZnO precursors have a direct band gap due to the correct dependence between  $(\alpha h\nu)^2$  and  $h\nu$  to obtain the energy band gap value. The results are shown in the table below. Note that energy band gap values for APr and EA at 300 °C have not been gotten because the absorption coefficient did not follow the dependence needed.

T (°C)	E <sub>g</sub> APr (eV)	E <sub>g</sub> AB (eV)	E <sub>g</sub> EA (eV)	E <sub>g</sub> AMB (eV)
300	-	3.00 ± 0.03	-	3.22 ± 0.01
400	3.18 ± 0.05	3.03 ± 0.01	3.19 ± 0.03	3.23 ± 0.02
500	3.23 ± 0.01	3.07 ± 0.06	3.22 ± 0.06	3.23 ± 0.02
600	3.22 ± 0.03	3.12 ± 0.05	3.25 ± 0.01	3.24 ± 0.01

TABLE 1: Energy band gap for all ZnO precursors at each annealing temperature.

Literature indicates that the energy band gap for pure ZnO is around 3.3 eV, but as we can see in table 1, all the values determined in the study are slightly lower. We can also notice that a general trend is followed for all precursors: the higher the annealing temperature, the larger the energy band gap. According to the literature, this could be due to the presence of contaminants that introduce shadow p-doping level into the bandgap [14].

Elemental analysis has given the appropriate information to analyse the energy band gap results and correlate them with impurities. As shown in Figure 1, the amino alcohols used in this study are classified in 2 different molecular structures: aliphatic (EA, APr and AMB) and aromatic (AB). Elemental analysis results for all the precursors that belong to the same molecular structure group are very similar, so we show below the results for one precursor of each one of these groups. A systematic uncertainty of ( $\pm 0.2$ ) has been added to the concentration values of all impurities.

T (°C)	N <sub>AB</sub> %	C <sub>AB</sub> %	H <sub>AB</sub> %	N <sub>APr</sub> %	C <sub>APr</sub> %	H <sub>APr</sub> %
300	2.2	32.2	3.5	1.3	12.0	1.3
400	4.3	29.3	2.0	1.0	5.8	0.7
500	0.6	7.1	0.9	0.1	0.8	0.1
600	0.4	3.5	0.0	0.1	0.3	0.0

TABLE 2: Elemental analysis for APr (aliphatic structure) and AB (aromatic structure), where N is Nitrogen, C is carbon and H is hydrogen.

As we can see in table 2, the samples used in this study have some impurities. The concentration of these impurities decreases as the annealing temperature increases, as expected. Furthermore, according to other studies, the presence of Nitrogen and Carbon decreases the energy band gap of ZnO [6,7]. Now we can conclude that band gap energies obtained are slightly lower than the one of pure ZnO because of the impurities present in the samples. As the concentration of impurities decreases, the energy band gap increases and approaches the band gap value of pure ZnO. We can also notice that AB has the lower energy band gap of all precursors at any temperature and this result correlates perfectly because it is the precursor with the higher concentration of impurities

due to his molecular structure. We can conclude that the aromatic ring is difficult to be released from our precursors by temperatures up to 600 °C, contrarily to the other linear structures.

Elemental analysis also shows a higher concentration of Zinc (Zn) in all samples compared to Oxygen (O), as shown in table below, what should lead to O vacancies. According to literature, O vacancies act like doping donors [8], so it is probable that all samples studied are n-type semiconductors.

Precursor	O %	Zn %
APr	24.2	32.8
AB	19.5	26.4
EA	26.1	35.3
AMB	21.2	28.8

TABLE 3: Oxygen and Zinc concentrations for all ZnO precursors.

Regarding photoluminescence, 2 different measurements have been analysed for each precursor. One of them after annealing at 300 °C and the other one after annealing at 600 °C. The different spectra obtained are represented below. AMB spectrums are not shown since PL data did not follow the correct dependence like the other precursors, probably due measurement mistake.

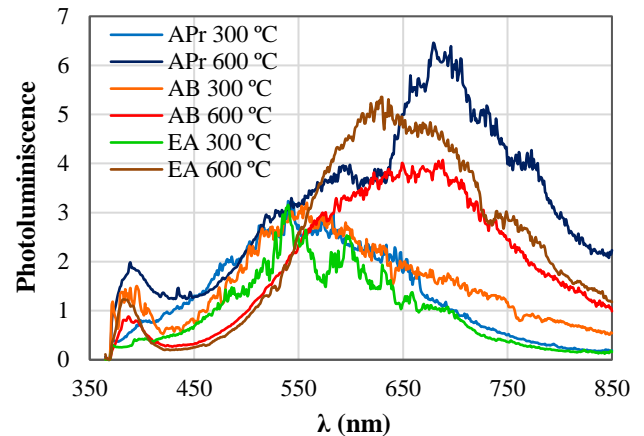


FIG. 4: Photoluminescence spectrum for APr, AB and EA at an annealing temperature of 300 °C and 600 °C.

All ZnO precursors exhibit 2 characteristic peaks, one in the near UV and the other in the visible region. The near UV peak is present in all samples at around 380 - 390 nm, regardless of the annealing temperature. This emission is thought to be due to excitonic recombination [15], a process where an electron in the CB is recombined with a hole in the VB. The energies corresponding to these peaks are around 3.1 - 3.2 eV, and seem to increase with annealing temperature, what matches well with the band gap energies obtained in UV-VIS spectroscopy.

The wavelength of the peaks present in the visible region depends strongly on annealing temperature. As we can see, samples heated at 300 °C generate emissions at around 550 nm, corresponding to green light, and samples heated at 600 °C generate emissions at around 620 - 700 nm, corresponding to orange and red light respectively.

The origin of the different luminescence emissions in the visible region has not been clarified yet. These emissions depend upon the synthesis procedure, morphology, impurities,

vacancies and surface defects. Typically, green luminescence has been attributed to radiative recombination of simple ionized oxygen vacancies [9]. This is very commonly observed in oxygen deficient ZnO, such as the samples used in this study (proved by elemental analysis). It is also thought that oxygen interstitial related defects are responsible for orange luminescence. Moreover, some studies have proved that the addition of carbon increases the oxygen vacancies in ZnO by the reduction reaction [10].

All this information correlates well with the results acquired in this study. As we have shown before, at low annealing temperatures, samples have a higher concentration of impurities (specially carbon), so there are more oxygen vacancies and green luminescence predominates. By contrast, at high annealing temperatures, samples have a very low concentration of impurities, so the number of oxygen vacancies are very low compared to oxygen interstitials and orange-red luminescence predominates. The reduction in the green emissions can also be attributed to the reduction of the deep level defects [10].

Besides, we can see that AB has the lowest PL intensity at 600 °C, probably because it is the precursor with the higher concentration of impurities at this annealing temperature. Furthermore, we can conclude that the increase of annealing temperature produces a significant improvement in the visible photoluminescence, as all 600 °C PL spectra have a much higher intensity than the 300 °C PL spectra.

Finally, SEM images of the samples were taken and are shown below. Images of 3 precursors at different annealing temperatures are enough to make the desired conclusions.

With this technique we have been able to ascertain that all ZnO precursors promote non-uniform layers, with an average thickness of the order of few microns. The thickness differs depending on the region of the layer due to these worm-like structures, which are probably composed of aggregates of ZnO monocrystals [1].

The images clearly show the molecular structure difference between aliphatic and aromatic amino alcohols used. Specially at low annealing temperatures, where samples have a high concentration of impurities, AB molecular structure is very different compared to APr and EA.

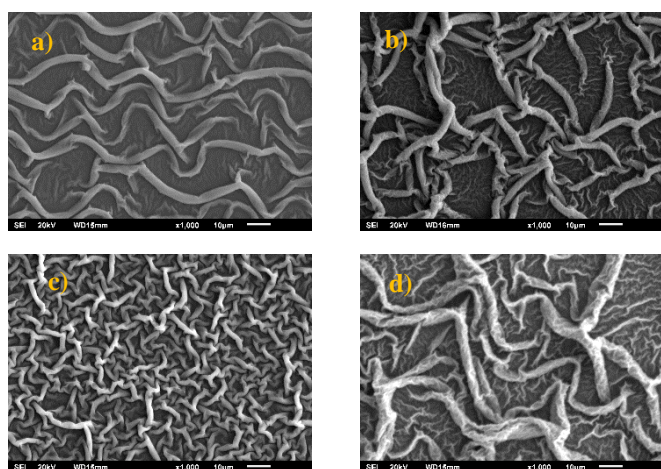


**FIG. 5:** SEM micrographs for APr at each annealing temperature: a) 300 °C, b) 400 °C, c) 500 °C and d) 600 °C.

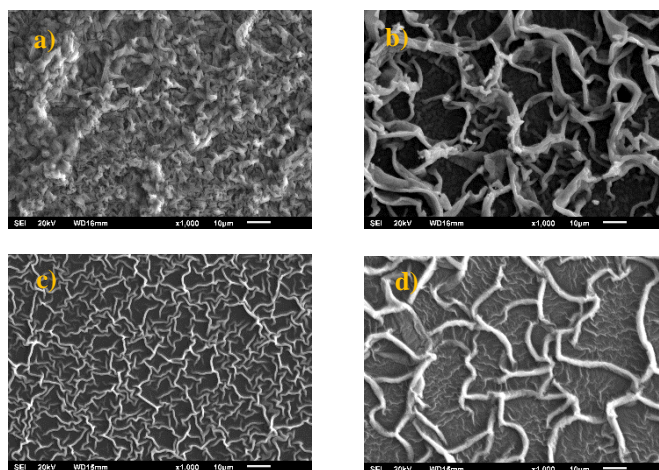


**FIG. 6:** SEM micrographs for AB at each annealing temperature: 00 °C, b) 400 °C, c) 500 °C and d) 600 °C.

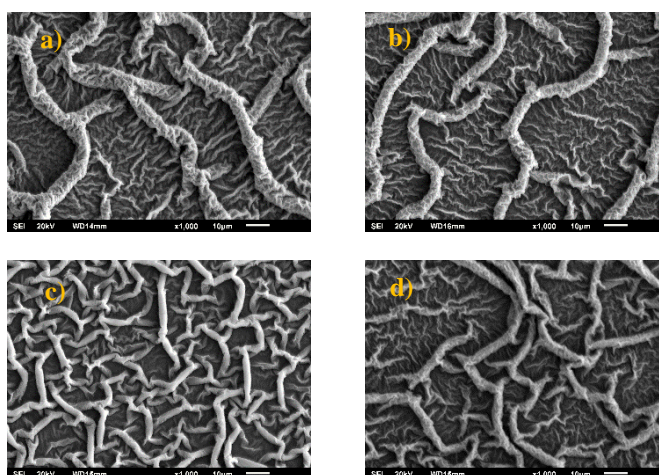


**FIG. 7:** SEM micrographs for EA at each annealing temperature: 00 °C, b) 400 °C, c) 500 °C and d) 600 °C.

We can also conclude that probably the most significant chemical change occurs between the annealing temperatures of 400 and 500 °C, due to the big molecular structure differences at these 2 temperatures. Between 300 – 400 °C and 500 – 600 °C samples seem to experience more like a physical change where particle size becomes bigger and the material improves his crystallinity.

### III. CONCLUSIONS

In the present study, optical and structural properties of ZnO precursors with different molecular structure (aliphatic and aromatic) were investigated. The energy band gap was determined from UV-VIS spectroscopy and found to vary between 3.00 – 3.25 eV, depending on the precursor and the annealing temperature. Elementary analysis has showed that, as the annealing temperature increases, the concentration of impurities decreases, and in consequence, the energy band gap increases and approaches the band gap value of pure ZnO (3.3 eV). From these techniques, we have also determined that all ZnO precursors possess direct band gap and Oxygen vacancies, what should lead to n-type semiconductors. Photoluminescence spectra presented two characteristic peaks

for each sample: one in the near UV due to excitonic recombination and related with the energy band gap found, and the other in the VIS region due to different structural defects. We have concluded that, as the concentration of impurities decreases, the VIS peak moves to a higher wavelength and the PL efficiency increases. SEM showed that all ZnO precursors promote non-uniform, worm-like layers and the structural difference between aliphatic and aromatic precursors. It has also been concluded that samples experience an important chemical change between the annealing temperatures of 400 and 500 °C, while they experience more like a physical change

between 300 – 400 °C and 500 – 600 °C, where particle size becomes bigger and the material improves his crystallinity.

### Acknowledgments

I would like to thank those who have contributed helpful discussions, support and encouragement, specially my advisor, Anna Vilà, for all his help and guidance. I also wish to express my gratitude to my family and friends, who have shared with me this journey.

- 
- [1] Alberto Gómez-Núñez, Pere Roura, Concepción López, Anna Vilà. Applied Surface science.
  - [2] Dr. B. Jill Venton – University of Virginia. Ultraviolet-Visible (UV-VIS) Spectroscopy.
  - [3] Belarusian State University – Tempus program. Study of semiconductors by UV-VIS spectroscopy.
  - [4] Davis, E. A; Mott, N. F. (1970). Conduction in non-crystalline systems V. Conductivity, optical absorption and photoconductivity in amorphous semiconductors.
  - [5] UCL School of Pharmacy. CHN Elemental Microanalysis.
  - [6] Xinyu Zhang, Jiaqian Qin, Ruru Hao, Limin Wang, Xi Shen, Richeng Yu, Sarintorn Limpanart, Mingzhen Ma, Riping Liu. Carbon-Doped ZnO Nanostructures: Facile Synthesis and Visible Light Photocatalytic Applications.
  - [7] Ping Lia, Sheng-hua Dengb, Yi-bao Lia, Li Zhanga, Guo-hong Liua, Jing Huangc. First-principles Study on Neutral Nitrogen Impurities in Zinc Oxide.
  - [8] D.M. Hofmann, D. Pfisterer, J. Sann, B.K. Meyer, R. Tena-Zaera, V. Munoz-Sanjose, T. Frank and G. Pensl. Properties of the oxygen vacancy in ZnO.
  - [9] Himanshi Gupta, Jitendra Singh, R. N. Dutt, Sunil Ojha, Soumen Kar, Ravi Kumar, V. R. Reddy and Fouran Singh. Defect-induced photoluminescence from gallium-doped zinc oxide thin films: influence of doping and energetic ion irradiation.
  - [10] Protima Rauwel, Martin Salumaa, Andres Asna, Augustinas Galeckas and Erwan Rauwel. A Review of the Synthesis and Photoluminescence Properties of Hybrid ZnO and Carbon Nanomaterials.
  - [11] Hayes G.R, Deveaud B. (2002). Is luminescence from quantum wells due to excitons? – Physica Status Solidi.
  - [12] Pavan M. V. Raja, Andrew R. Barron. Physical Methods in Chemistry and Nano Science.
  - [13] Kalsoom Akhtar, Shahid Ali Khan, Sher Bahadar Khan and Abdullah M. Asiri. Scanning Electron Microscopy: principle and applications in nanomaterials characterization.
  - [14] Bharati Panigraphy and D. Bahadur. P-type Phosphorus doped ZnO nanostructures: an electrical, optical and magnetic properties study.
  - [15] Dinesh Thapa, Jesse Huso, John L. Morrison, Caleb D. Corolewski, Matthew D. McCluskey and Leah Bergman. Achieving highly-enhanced UV photoluminescence and its origin in ZnO nanocrystalline films.
  - [16] K.D.Vernon-Parry. Scanning electron microscopy: an introduction.